# REVIEW ARTICLE

# Space-based magnetometers

Mario H. Acuña[a]

*Laboratory for Extraterrestrial Physics, NASA Goddard Space Flight Center, Code 695, Greenbelt, Maryland 20771*

The general characteristics and system level concepts for space-based magnetometers are presented to illustrate the instruments, principles, and tools involved in making accurate magnetic field measurements in space. Special consideration is given to the most important practical problems that need to be solved to ensure the accuracy of the measurements and their overall impact on system design and mission costs. Several types of instruments used to measure magnetic fields aboard spacecraft and their capabilities and limitations are described according to whether they measure scalar or vector fields. The very large dynamic range associated with magnetic fields of natural origin generally dictates the use of optimized designs for each particular space mission although some wide-range, multimission magnetometers have been developed and used. Earth-field magnetic mapping missions are the most demanding in terms of absolute accuracy and resolution, approaching $<1$ part in $100\,000$ in magnitude and a few arcsec in direction. The difficulties of performing sensitive measurements aboard spacecraft, which may not be magnetically clean, represent a fundamental problem which must be addressed immediately at the planning stages of any space mission that includes these measurements. The use of long, deployable booms to separate the sensors from the sources of magnetic contamination, and their impact on system design are discussed. The dual magnetometer technique, which allows the separation of fields of external and spacecraft origin, represents an important space magnetometry tool which can result in significant savings in complex contemporary spacecraft built with minimum magnetic constraints. Techniques for in-flight estimation of magnetometer biases and sensor alignment are discussed briefly, and highlight some basic considerations within the scope and complexity of magnetic field data processing and reduction. The emerging field of space weather is also discussed, including the essential role that space-based magnetic field measurements play in this complex science, which is just in its infancy. Finally, some considerations for the future of space-based magnetometers are presented. Miniature, mass produced sensors based on magnetoresistance effects and micromachined structures have made significant advances in sensitivity but have yet to reach the performance level required for accurate space measurements. The miniaturization of spacecraft and instruments to reduce launch costs usually results in significantly increased magnetic contamination problems and degraded instrument performance parameters, a challenge that has yet to be solved satisfactorily for ''world-class'' science missions. The rapidly disappearing manufacturing capabilities for high-grade, low noise, soft magnetic materials of the Permalloy family is a cause of concern for the development of high performance fluxgate magnetometers for future space missions. [DOI: 10.1063/1.1510570]

## I. INTRODUCTION

Magnetometry is the science of accurate measurements of the strength and direction of magnetic fields and space magnetometry represents the specialized science of making magnetic field measurements in space, aboard vehicles such as rockets, balloons, and spacecraft. The Chinese are reported to have been the first to use the Earth's magnetic field for navigation purposes. More than 4500 years ago they used splinters of magnetite as compasses for direction finding, and

Marco Polo is credited with taking this information to Europe in the 13th century. Some 300 years later, Sir William Gilbert, in ''De Magnete,'' was the first to describe the Earth as a ''giant magnet'' and Gauss developed the mathematical tools for its analytical representation. We now know that magnetic fields are omnipresent in nature and just about every major body in the solar system has magnetic fields associated with it, either of interior origin, induced, or remanent. The interplanetary magnetic field is the extension into space of the Sun's magnetic field carried outwards by the supersonic flow of the solar wind. Sources of magnetic fields include electrical currents circulating in fluids, conductors, and

[a]Electronic mail: mario.acuna.1@gsfc.nasa.gov

     3717

ionized gases, ''permanent'' magnets like those that occur naturally (magnetite or lodestone) and those made industrially of materials like iron, iron oxides, cobalt, nickel alloys, and rare earth compounds.

The beginnings of space magnetometry trace back to measurements of the Earth's magnetic field with instruments flown on balloons and rockets in the early 1950s. The measurement techniques used in these experiments were largely adapted from instruments developed around the time of World War II, when magnetometers were widely used in geophysical applications, navigation, salvage, and mine and antisubmarine warfare. The early space probes made significant discoveries: the Earth's magnetosphere, the comet-tail-like geometry of the antisunward Earth's magnetic field, the interplanetary magnetic field (IMF), its sector structure, and the many boundaries associated with the interaction of the Earth's magnetic field with the solar wind. Dolginov et al.,[1–3] Sonnet,[4] Heppner et al.,[5] Cahill,[6] and Ness[7,8] were among the first investigators to equip rockets and satellites with magnetometers and carry out measurements in the Earth's ionosphere and magnetosphere in the interplanetary medium and around the Moon.

Why is magnetometry so important in space exploration? Magnetic field measurements are essential to organize and understand energetic charged particle and plasma measurements and to derive fundamental information about the environment surrounding different bodies in the solar system. Charged particles move easily along magnetic field lines because their transverse motion is opposed by the Lorenz force. Knowing the geometry of the field is equivalent to having a map of the pathways followed by the particles' guiding center. Magnetic field measurements also represent one of the few remote sensing tools used by spacecraft (gravity being another) that provide information about the *deep interior* of a planet rather than just its surface and/or atmosphere which are customarily studied with multispectral imaging instruments. Planetary magnetic fields like those of the Earth, Jupiter, and Saturn are generated by currents circulating in their liquid metallic cores or perhaps the core–mantle interface. The primary energy source powering these dynamos is thermal convection of electrically conducting fluids driven by the internal heat flux and organized by planetary rotation. The outermost giant planets Uranus and Neptune are not assumed to have formed metallic cores and their magnetic fields are generated closer to the surface, where electrical currents can flow in high-conductivity crustal "oceans." [9–12] In the case of the terrestrial planets, Venus does not possess an intrinsic magnetic field[13] while Mercury is believed to be currently magnetized by the remains of an ancient dynamo which is decaying over time.[14] The study of the Hermean field is one of the primary objectives of the MESSENGER and Beppi Colombo missions that will be launched in the 2003–2005 time frame.[15,16] The existence of an intrinsic magnetic field at Mars was a topic of considerable discussion.[17–19] Recent measurements by the Mars Global Surveyor (MGS) Mission not only demonstrated that Mars does not currently possess an internal field, but made the remarkable discovery of the existence of strong crustal magnetic fields of paleomagnetic origin.[20–22] In many areas

the martian field is organized in linear structures and is closely correlated with the age of the crustal terrain. The Lunar Prospector (LP) mission[23–25] provided a new and detailed view of the lunar, crustal magnetic fields discovered by the Apollo missions.[26–31] These are correlated in a puzzling way to the antipodes of the great impacts that created the lunar basins. The MGS and LP magnetic field observations are revolutionizing our thinking about the early history and thermal evolution of Mars and the Moon. They are certain to result in significant revisions of our views of Earth's magnetic anomalies and their origin. The role played by giant impacts during the formation and early evolution of the solar system has now achieved a new level of relevance in our limited understanding of the processes that took place more than four billion years ago.

Planetary space missions such as Pioneer 10 and 11, Pioneer Venus, the Mariner series, Voyager, Helios, Ulysses, Giotto, Mars Global Surveyor, Galileo, and NEAR have carried out magnetic field measurements in the immediate vicinity of most of the planets in the solar system, as well as around comets and asteroids.[32–41] The NEAR–Shoemaker spacecraft was placed in orbit around the asteroid 433 Eros on 14 February 2000 and spent one year making magnetic field measurements from 35 and 50 km orbits. On 12 February 2001 the spacecraft landed on 433 Eros and continued to make magnetic field observations from the surface for several days.[33,42–44] Contrary to expectations based on measurements and analyses carried out at asteroids Braille and Gaspra by Deep Space-1 and Galileo,[36,38] no magnetic field of asteroidal origin was detected, making 433 Eros a remarkably nonmagnetic, undifferentiated primitive object.[42] The weak IMF has been measured by spacecraft such as the Interplanetary Monitoring Platform (IMP) series, Pioneers, Voyager, Mariner, WIND, ACE, GEOTAIL, and many others.[8,40,45,46] A recent review of the history of vector magnetometry in space was given by Snare.[47] Magnetic field measurements are used as well in many Earth-orbiting spacecraft for engineering applications. These include attitude determination and control, spacecraft momentum management, and scientific instruments pointing.[48,49] The Earth's magnetic field provides a convenient "natural" frame of reference, which can be modeled with good accuracy, and modern systems and spacecraft utilize it to establish their orientation and activate control systems. Where absolute angular measurement accuracy of the order of $1°–2°$ degrees is acceptable, magnetic systems provide significant cost, simplicity, and reliability advantages over inertial sensor-based systems. A common space-based application of magnetometers aboard spacecraft in low and geostationary Earth orbit is the control of electromagnets which, when energized, apply torque to the spacecraft by interacting with the geomagnetic field. These "magnetic torquers" are generally used to "desaturate" momentum wheels (reduce the accumulated angular momentum resulting from the operation of reaction wheels aboard a spacecraft) or to orient the spacecraft along a desired direction.[48–50]

Numerous discoveries have been made studying the sources, geometry, and temporal behavior of solar system magnetic fields but there is still much to be learned. In recent

years the new field of "space weather" has evolved from the extended, multipoint observations of the Sun–Earth environment that have been carried by international collaborative programs such as the International Solar-Terrestrial Physics (ISTP) Program since 1992 that utilize multiple spacecraft and ground-based systems.[51,52] Solar transient events such as coronal mass ejections (CMEs), solar flares, and magnetic clouds can affect operation and even cause failure in Earth-orbiting spacecraft and power distribution systems on the ground such as the North American power grid.[53–58] The reliable operation of contemporary telecommunications, global positioning, and strategic satellites today depends to a significant extent on near-real time knowledge of space weather conditions. The prevention of power grid failures and associated large area blackouts in North America and northern Europe which are caused by ground currents in transmission lines induced by the time-varying geomagnetic field and can destroy distribution transformers, is also dependent upon timely access to space weather information.[59–61] Space magnetometry is now an established and mature science which plays a critical role in the activities described above and is expected to remain so for the foreseeable future. In the US, the National Space Weather Program, NASA's Living with a Star (LWS) program and the Sun–Earth Connection research efforts, including NASA's Solar Terrestrial Probes, all rely on space magnetometry as one of the key measurements to be carried out. Similar programs in Europe, Russia, and Japan reflect the essential importance of magnetic field measurements in space.[62–66]

The magnetic field measurement techniques and instruments described in this review date from the late 1930s until the present time. Important sensor developments took place in the 1936–1955 time frame such as the invention of the fluxgate[67] and the application of nuclear magnetic resonance to magnetometry. The traditional definition of space-based "magnetometry" does not include the sensing of time-variable magnetic fields by induction sensors such as search coils, which will not be discussed in this review. Contemporary advances in wide-dynamic-range magnetic field sensing technology have focused on improvements in sensor noise performance, analog and digital signal processing techniques, as well as instrument miniaturization. Modern, high volume magnetic field sensing technologies, e.g., anisotropic magnetoresistance (AMR), giant magnetoresistance (GMR), and micromachined devices (MEMS), have yet to compete effectively with established sensors in space applications. Devices based on magnetoresistance effects (AMR and GMR), although they offer adequate sensitivity for Earth-field sensing, suffer from problems like hysteresis and poor stability that are introduced by the use of "flux concentrators" or biasing arrangements to enhance the output signal or to linearize the transfer function.[49,68] Magnetometers using superconducting quantum interference devices (SQUIDs) can exhibit significantly increased sensitivity over those described here, but the complex logistics of cryogens and associated systems have prevented their application to space-based measurements.[49]

The primary emphasis of this review is on considerations at the space systems level rather than detailed discussion of individual sensing technologies. The reason for this approach is that the latter are reasonably well developed and have been extensively reviewed in the literature.[8,49,69] On the other hand, system level trade-offs, which determine the ultimate success or failure of magnetic field measurements on a given space mission, have not received equal attention. Spacecraft, components, and instrument design philosophies have changed significantly in the last 20 years, particularly with respect to the use of "heritage" or "off-the-shelf" subsystems to reduce development costs. To ensure the accuracy of magnetic field measurements, space vehicles have to be designed to minimize the generation of undesirable static and dynamic fields, regardless of the type of sensor used, and these requirements are seldom met by low cost, readily available components. The magnetic signature reduction process affects all aspects of spacecraft, instruments, and mission design and can have a dramatic impact on the cost and schedule and even the viability of sensitive magnetic field measurements, if not addressed early and correctly in the development cycle.

## II. MEASURING MAGNETIC FORCES

The magnetic force between two magnetic poles is given by an expression identical to that of the gravitational force between two masses,

$$\mathbf{F} = (m_1 m_2 / \mu r^2)\mathbf{r}, \tag{1}$$

where $\mathbf{F}$ is the force in dynes [centimeter-gram-second (cgs) system] between the poles that are separated by $r$ cm ($\mathbf{r}$ is the unit vector directed between $m_1$ and $m_2$). The permeability of the medium is denoted by $\mu$. Since the lines of force are closed, magnetic poles cannot exist by themselves and always exist in pairs ($\nabla \cdot \mathbf{B} = 0$), while the force between them can be repulsive or attractive depending on the polarity of the poles involved.

The magnetic quantities derived are the *magnetic field strength* $\mathbf{H}$, which is defined as the force $\mathbf{F}$ per unit pole and is measured in oersteds (cgs), and the *magnetic field induction*, which is the field $\mathbf{B}$ induced by the excitation $\mathbf{H}$ in a medium of permeability $\mu$,

$$\mathbf{B} = \mu \mathbf{H}. \tag{2}$$

In the cgs system of units, $\mathbf{B}$ is measured in gauss. In air or vacuum, the permeability $\mu$ is unity so for all practical applications in space oersted and gauss can be used interchangeably. In the Systeme International (SI) of units, the magnetic induction is measured in tesla ($10^4$ G), while the magnetic field strength is measured in ampere/turns/cm. The permeability of air (vacuum) in the SI system is $\mu = 4\pi \times 10^{-7}$. To quantify weak magnetic fields the nanotesla (1 nT $= 10^{-9}$ T) and the older, equivalent cgs unit the gamma (1 $\gamma = 10^{-5}$ G $= 1$ nT) are frequently used interchangeably. The Earth's magnetic field at the surface and near the equator has an approximate strength of 31 000 nT or 0.31 G, whereas Jupiter's north magnetic pole field strength is more than 14 G or 1 400 000 nT. Solar magnetic fields associated with coronal loops and prominences can reach values as high as several thousand Gauss. At the opposite

end of the dynamic range, the IMF at the Earth's orbit [1 astronomical unit (AU)] is typically of the order of 5–10 nT, while at the orbit of Uranus and Neptune it may be as low as 0.05 nT or, equivalently, $5 \times 10^{-11}$ G. This very large dynamic range of magnetic field intensities presents unique challenges to the design of magnetic field instrumentation for space missions to the outer planets.

## III. MAGNETIC FIELD MEASURING INSTRUMENTS

As already introduced in the above paragraphs, the instruments used to measure the strength (and direction) of the magnetic field are called *magnetometers*. Since the magnetic field is a *vector* quantity that has both magnitude and direction, we usually differentiate between two generic classes of instruments:

(a) **scalar** magnetometers, which measure only the total strength or magnitude of the ambient magnetic field regardless of its orientation, and

(b) **vector** magnetometers, which produce an output proportional to the strength and direction of the magnetic field, referenced to a principal axis in the sensing element. The polarity or sign of the output in general depends on the direction of the ambient field with respect to the magnetometer sensing axes.

Both classes of instruments have been used for space measurements but vector magnetometers are far more common due to their capability of providing directional information. This is essential for understanding of the physical phenomena being studied or for the intended application in attitude determination and control. We will discuss below some of the principal characteristics of these instruments, their advantages and limitations, and the challenging problem of performing sensitive magnetic field measurements aboard space platforms such as spacecraft, planetary probes, rockets, and balloons. For a comprehensive review of early space research magnetometers and techniques, see the review by Ness,[8] and references therein.

### A. Scalar magnetometers

The most common scalar magnetic field measuring instrument in general use is the *proton precession magnetometer*, which is based on the phenomenon of nuclear magnetic resonance. At the end of World War II it was discovered that many atoms possess a net magnetic moment and behave as small magnets. A sample of a liquid rich in protons (hydrogen nuclei) surrounded by a coil is magnetically polarized to align all of its magnetic moments in a given direction. The sample is then allowed to "relax" in the presence of an external magnetic field. The protons that have been aligned parallel to the polarizing field will precess like spinning tops around the ambient magnetic field and induce an ac signal in the polarizing coil whose frequency is proportional to the magnitude of the field. This frequency is called the Larmor frequency and is given by

$$f \ (\mathrm{Hz}) = (\tau_p B / 2\pi), \tag{3}$$

where $B$ is the magnitude of the external field and the proportionality constant $\tau_p$ is the *gyromagnetic ratio* of the proton. This is the ratio of the proton's magnetic moment to its spin angular momentum. The value of $(2\pi/\tau_p)$ is known very accurately from quantum mechanical principles, 23.4874 (nT/Hz), and the proton precession magnetometer is the primary standard used in the calibration of other magnetometers and coil systems.

The basic proton precession magnetometer is therefore composed of a liquid sample rich in protons (water, naphta, kerosene, etc.), a polarizing/sensing coil that surrounds the sample, an ac amplifier, and a duty cycled current source, which are alternatively connected to the coil. After being used to polarize the sample the coil is connected to the amplifier to sense the Larmor signal, which lasts only a few seconds and whose frequency is then measured with an ordinary computing counter. The polarize/count cycle of conventional proton precession magnetometer designs is typically 1 s or more. The liquid sample volume is relatively large and massive, particularly when the polarizing coil mass is considered, and liquids that can operate over a wide temperature range are required. The power required to generate the 100 G or more polarizing field is appreciable, and useful signals can only be obtained for ambient fields larger than approximately 20 000 nT and only if the local spatial field gradient is small. These limitations have restricted the use of traditional proton precession instruments for space measurements to a few, very specialized applications such as sounding rockets and balloons (see Ref. 49, and references therein).

Recent improvements to this basic sensing technique, like the Overhauser effect proton precession magnetometer, use an indirect technique to "polarize" the sample much more efficiently and can generate a continuous Larmor precession signal.[65,66,70] The proton-rich liquid sample is doped with a free radical as a source of electrons which are pumped with rf energy at ~20–60 MHz. The electrons are effectively coupled to the protons in the sample, which are then polarized dynamically by the rf excitation. This method of polarization is much more efficient than the dc method (a few watts versus tens of watts) and yields Larmor signal amplitudes which are 100 times larger, allowing continuous measurements to be made with sensitivity of ~ 0.02 nT.

Optically pumped magnetometers are another class of magnetic field measuring instruments which have found application in space measurements, both as scalar as well as vector instruments.[41,71–74] In the scalar configuration, they are capable of measuring magnetic fields over a wider range than the proton precession instruments and with much higher time resolution. These instruments use the energy required to transfer atomic electrons from one energy level to another as the mechanism for magnetic field detection. A cell containing a suitable gas is irradiated with light from a discharge lamp at the proper frequency to excite the atoms to a quantum level, which becomes overpopulated as a consequence of forbidden transitions in the system. Under these conditions, the gas cell becomes transparent to the irradiating beam (the process used to achieve this is called optical pumping). If the cell is then subjected to a rf signal with energy appropriate to
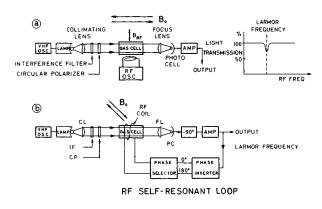
FIG. 1. Schematic for an optically pumped magnetometer (after Ref. 8): (a) basic configuration and (b) self-oscillating loop.



FIG. 2. Two-cell optically pumped scalar magnetometer sensor (after Ref. 8): (a) schematic of the arrangement and (b) physical arrangement of the sensors required to avoid "null" zones.

cause depopulation of this energy level, it will become opaque again and, block the transmission of light at the discharge lamp frequency. The most commonly used elements for optically pumped magnetometers are helium and alkali metals like cesium, rubidium, and sodium. Helium and its isotopes in particular are in wide use in high accuracy, high time resolution scalar magnetic field measurements for military applications. Modified versions of these "metastable helium" magnetometers were developed to perform wide dynamic range scalar and vector measurements aboard spacecraft and are described briefly below in Sec. III B.[41,64,71,75]
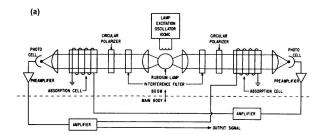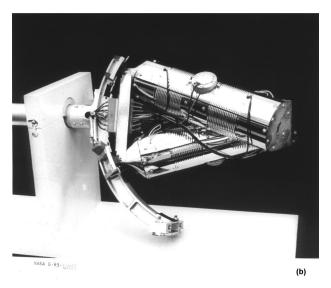
A generic optically pumped magnetometer is illustrated in Fig. 1. It consists of a discharge lamp, which irradiates one end of a gas cell containing the element chosen in gaseous form through a system of filters and polarizers. At the opposite end, a solid state photodetector measures the intensity of the incident light. The electrons in the gas cell will precess about the axis of the external magnetic field at the Larmor frequency of the chosen element, and modulate the intensity of the light incident upon the photodetector at the same rate. Thus, the output from the photodetector is an ac signal at the Larmor frequency given by

$$f = \tau_e B / 2\pi, \tag{4}$$

where $\tau_e$ is the *electron* gyromagnetic ratio for the chosen element. For helium ($\tau_e/2\pi$) corresponds to 28 (Hz/nT), considerably larger than the value of 0.042 576 02 (Hz/nT) obtained from proton precession instruments, making possible higher time resolution measurements. The corresponding figures for cesium and rubidium are 7 and 4.67 (Hz/nT), respectively.

The output of the photodetector is amplified and fed back to a coil wound on the cell, causing the system to oscillate continuously at the Larmor frequency. Because of the high frequencies involved, it is possible to measure very small magnetic field variations ($\geqslant 0.01$ nT) superimposed on large background fields.

If the external magnetic field is aligned with the axis of the gas cell the amplitude of the Larmor signal decreases to a minimum, giving rise to the appearance of "null zones." For this reason most optically pumped scalar magnetometers used for space measurements utilize two cells oriented at different angles to fill in the null zones associated with each

detector.[8] A typical two-cell sensor arrangement is shown in Figs. 2(a) and 2(b). Another important issue associated with these magnetometers is the use of high-level rf signals for optical pumping. These need to be carefully controlled and shielded to avoid interference with vector magnetometers and sensitive electronics, communications, and other spacecraft systems. The high power dissipation and associated thermal flux and to the use of nonmagnetic metallic shields around the sensor will often give rise to significant measurement errors associated with thermoelectric currents due to Thompson and Seebeck effects.

Scalar magnetometers of the types described above have a typical dynamic range of 20 000–70 000 nT and cannot be used to measure weak fields such as those associated with the interplanetary medium, the Moon, Mars, Venus, or Mercury. Their principal use is in low Earth orbit and in conjunction with vector magnetometers to acquire very accurate magnetic field mapping data.[65] The Cassini mission to Saturn included a scalar helium magnetometer to map this planet's remarkable axisymmetric field.[64] A scalar magnetometer is often used as an absolute calibration tool in conjunction with a vector magnetometer to allow real time determination of correction factors. Laboratory-based proton precession magnetometers are routinely used as primary calibration standards.

The mass and power consumption associated with scalar magnetometers can be significant. Classical proton precession magnetometers may draw several tens of watts during the polarizing cycle while the mass of the sensor alone may

exceed 1 kg and that of the electronics 2–3 kg. Helium, rubidium, and cesium magnetometers require significant rf power for excitation, with 10–15 W being typical figures. The high levels of rf present in these instruments also require close attention to shielding and the prevention of generation of local magnetic fields by rectification or thermoelectric effects. The Overhauser and helium scalar magnetometers mass and power requirements can be reduced to a few watts and 1–2 kg with modern components and specialized design techniques.[65,66] The typical noise performance of these instruments is in the range of 0.01–0.03 nT root mean square (rms) over a bandwidth of 0–1 Hz, and the practical upper limit to their dynamic range is $\sim 1.5-2 \times 10^5$ nT, an important consideration for missions to planets with strong magnetic fields like Jupiter.

## B. Vector magnetometers

Vector magnetometers are, by a very large margin, the most widely used type of instrument for magnetic field measurements in space. In addition to providing information about the strength of the ambient field they also measure its direction and sense. Triaxial orthogonal arrangements of single axis sensors are used to measure the three components of the ambient field in a coordinate system aligned with the sensor magnetic axes. In contrast to proton precession and optically pumped *scalar* magnetometers whose accuracy is determined by quantum mechanical constants, vector magnetometers must be calibrated using accurately generated magnetic fields, both in strength and direction, at specialized facilities. The magnetometer output for the zero applied field, scale factor, and stability over temperature and time depends on electrical component values which may drift as the instruments age or are exposed to effects of the space environment.[8,76–80] The alignment of the sensors may change as thermal or vacuum induced stresses deform the supporting structures or reference coordinate systems.[77,81,82] In spite of these challenges, extremely reliable, low power ($<1$ W) high performance vector instruments capable of measuring magnetic fields over a very large dynamic range, $<5 \times 10^{-3}$ to over $2 \times 10^6$ nT, were developed in the early 1970s for outer planets exploration.[35,41,83] They are capable of operating over a wide temperature range and have proven to be extremely radiation tolerant. Ultraprecise vector instruments with arc-sec resolution have also been used to map the Earth's magnetic field from orbit with unprecedented accuracy, both in magnitude as well as in direction.[77,79,84,85] The CLUSTER II mission launched in August of 2000[86] included a complement of four spacecraft flying in formation, each incorporating dual, high performance fluxgate magnetometers designed to make three-dimensional measurements of the ambient magnetic field.[62] One of the primary objectives of that mission's magnetic field instrumentation was to obtain, for the first time, measurements of local currents through the relation $\mathbf{J} = \nabla \times \mathbf{B}$.

The fluxgate magnetometer, which was invented by Aschenbrenner and Goubau[67] and developed during World War II as a submarine detector,[69,87] is the most common type of instrument used in space platforms. This type of sensor is
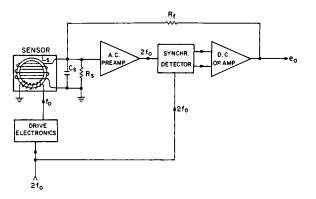


FIG. 3. Block diagram of a generic, single axis fluxgate magnetometer. A tuned single axis ring core sensor is shown.

also widely used in countless industrial, military, and scientific applications. The fluxgate sensor, as its name implies, is a device which is used to ''gate'' the ambient magnetic flux threading a sensing coil, converting it from a time stationary field into a time varying field. The latter gives rise to induced voltage in a sensing coil proportional to the strength and direction of the field. Gating of the ambient field is accomplished by driving cyclically to saturation a high permeability, nonlinear magnetic core with a large amplitude excitation signal. A differential coil wound around the core and the excitation coil is used to sense the output signal. When the core material is in the saturated state its permeability is very low and the total magnetic flux threaded by the sensing coil is not very different from that which would exist in free space. However, when the core is in its high permeability state, the flux threaded through it and the pick-up coil is greatly increased depending on the effective permeability of the core (and core geometrical shape). Thus, by cyclically switching the core in and out of saturation at frequency $f$, the ambient magnetic flux will be modulated at twice this frequency and a corresponding ac voltage will appear at the terminals of the sensing coil. The amplitude of this signal is proportional to the magnitude and direction of the ambient field, and its phase with respect to the excitation signal ($0°$ or $180°$) will depend on the sense of the field. In general, balanced core arrangements are used to prevent the excitation signal from appearing at the pick-up coil and to avoid generating a large signal at the excitation frequency. Many fluxgate sensor geometries have been used for space-based instruments, from commercial sensors using proprietary helical high permeability cores to sensors using ultralow noise ring cores developed by government laboratories. The very high performance of the latter has made them the sensors of choice for advanced space missions.[8,49,69,76,88–94]

A block diagram of a typical fluxgate magnetometer is shown in Fig. 3. A reference signal at frequency $2 f_0$ is derived from a stable oscillator and applied to a divider, from which the excitation signal at frequency $f_0$ is used to drive the sensor toward saturation (in this case a ring core sensor with a toroidal excitation winding). A differential sensing coil is wound around the outside of the ring core and, in most applications, tuned to the second harmonic of the drive frequency, $2 f_0$. Thus, if both core halves are identical, no signal at the excitation frequency will appear at the sense wind-

ing terminals. The presence of an external magnetic field will cause the appearance of a signal at frequency $2f_0$ and other even harmonics of the excitation frequency at the terminals of the sensing coil. This is due to the fact that one half of the ring core will not be balanced with respect to the other, similar to operation of a balanced modulator. This signal is amplified by the tuned ac preamplifier and applied to the synchronous detector or "lock-in" system. The magnitude of the output of this detector is proportional to the amplitude of the signal present at the output of the preamplifier, whereas the polarity of the output depends on the phase of the input signal with respect to the reference frequency $2f_0$. The output of the synchronous detector is then applied to a high gain integrating dc amplifier whose output is used to generate a current, which is fed back to the sense winding in the fluxgate sensor. The feedback current flowing through the sensing coil produces a magnetic field that opposes (and cancels almost completely) the original external field and the fluxgate sensor is used essentially as a null detector. This feedback arrangement yields an instrument with excellent linearity whose dc response is given by
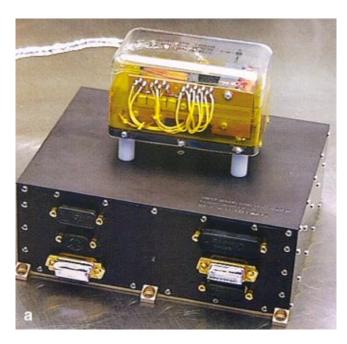
$$e_0(B, \theta) = kR_f B \cos(\theta) + V_z, \tag{5}$$

where $e_0(B, \theta)$ is the output voltage, $k$ is a constant related to the physical characteristics of the sensing coil with dimensions given in [ampere/Gauss], $R_f$ is the value of the feedback resistor, $B$ is the scalar magnitude of the field applied, and $\theta$ is the angle between the magnetic axis of the fluxgate sensor and the direction of the external field. $V_z$ is a small dc offset voltage, which is present when the external field is zero and is produced by asymmetries, offsets, and imbalances in the system. The magnetometer scale factor can be easily modified by changing the value of $R_f$ and this is done in instruments that must cover a large dynamic range like those used in the Voyager, MGS, ACE, WIND, and LP missions.[32,45,46,83] For a feedback system with a single integrator the transfer function is given by

$$H(s) = 1/[(s^2/\omega_n^2) + 2s(k/\omega_n) + 1], \tag{6}$$

where $\omega_n$ and $k$ are the characteristic natural frequency and damping factor of a second order system, respectively. The latter is directly proportional to the value of $R_f$ and inversely proportional to the ac gain in the system so simultaneous adjustments need to be made to the open loop gain and time constants to preserve the stability of the feedback loop for all scale factors selected.

Mass and power requirements for fluxgate magnetometers are significantly reduced with respect to those associated with scalar instruments. Typical general purpose, fluxgate magnetometers for attitude sensing and control require <0.5 kg and <0.5 W, respectively, with miniature units widely available. The latter integrate the sensor with the electronics in a single package, which is not necessarily an optimal arrangement for all applications as will be discussed below. Space research-grade instruments that incorporate wide dynamic range capabilities and advanced digital processing techniques have been built and they consume as little as 1 W and weigh 1 kg per unit.[34,37,45,62,83] Duty-cycled instruments have also been developed that draw just a few microwatts
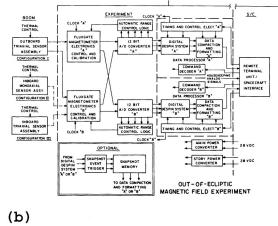




(b)

FIG. 4. (Color) Typical vector magnetometer instruments. (a) The sensor seen on top of the electronics box is mounted remote from the spacecraft bus, typically on a deployable boom. (b) Block diagram of a high performance, space-based magnetometer system. Note the extensive use of redundant systems to ensure reliability in missions of long duration.

average power at a sample rate of 1–2 samples/s. Figure 4(a) shows a typical high performance magnetic field instrument comprising a triaxial sensor assembly and an electronics box, which includes signal, data processing, and spacecraft interface circuits. The sensor shown on the top of the electronics box in Fig. 4(a) is mounted far from the spacecraft bus to minimize magnetic interference from spacecraft systems and other instruments. A block diagram, which illustrates the typical elements of a fully redundant instrument used for planetary exploration, is shown in Fig. 4(b).

A second type of vector instrument that has been used in a few planetary spacecraft is the Vector helium magnetometer.[41,71,75] Its operating principles are the same as those of the optically pumped magnetometers described earlier in Sec. III A, except that a Helmholtz coil system around the gas cell has been added. This coil system is used to generate synchronous sweep fields in two orthogonal planes that intersect along the optical axis by means of an auxiliary

electronic system. These sweep fields produce synchronous modulation in the photodetector light output, which can be used to derive vector information about the external magnetic field. Typically, a frequency of 200 Hz is used for the sweep field and the resulting signal at the photodetector is amplified, synchronously rectified, and the current fed back to the sensor assembly to cancel out the field applied. The operation is very similar to that implemented in a fluxgate magnetometer. Some differences are that the excitation and signal frequencies are identical and vector information is derived not from individual sensors but from sweeping fields applied to a common sensor along two orthogonal planes. The directions of the sensing "axes" are thus derived electronically and are not uniquely related to the mechanical alignment of individual sensors, as in fluxgates. The transfer function of the vector helium magnetometer (VHM) is identical to that of the fluxgate magnetometer given by Eq. (5). The mass and power requirements of VHMs are still higher than comparable performance fluxgate magnetometers with 2–3 kg and 4–6 W being representative figures. The power required to generate the sweep fields over the volume of the cell and increasing transfer function nonlinearity limit the upper limit measurement capability to $\sim 1.5 \times 10^5$ nT. As is the case for all optically pumped magnetometers, the lifetime of the gas cell and the stability of the light source are most important considerations for missions of long duration ($>3$–5 yr). In 1978–1979 NASA funded Scintrex, Canada, to study the aging process of cesium vapor lamps for the MAGSAT mission. It was concluded that lifetimes of the order of "several years" could be achieved under a stable thermal regime which maintained the lamp stem at 50 °C and the lamp envelope some 150–160 °C hotter. New techniques in striking the lamps and bringing them to their stable operating point were also necessary to extend their operational life. In the case of helium magnetometers, like those on the Pioneer 10 and 11 missions, the cell and lamp were constructed using special glass and seals to minimize gas leakage.

The stability of the zero level or bias over time and temperature and the noise performance of a vector magnetometer are some of the most important performance parameters to be considered for weak field measurements such as those of the IMF, the distant terrestrial magnetosphere, and around unmagnetized bodies. The data reduction and analysis effort associated with weak field magnetic field investigations are traditionally dominated by "zero level" determination issues. The scale factors and intrinsic sensor alignment are stable and once calibrated remain largely constant for the life of the mission. The noise power spectral density of a high performance fluxgate magnetometer is typical of "shot noise" devices and characterized by a $1/f$ spectrum with a typical value of $\sim 10^{-5}$ (nT$^2$/Hz) at 1 Hz for space research-grade instruments. The source of the noise is attributed to Barkhausen-like mechanisms that affect the motion of domains in ferromagnetic material in the sensor cores.[49] The absence of ferromagnetic materials in optically pumped magnetometers results in a flat noise spectrum for these devices and, in principle, improved long term stability over fluxgates. However, and for reasons discussed else-

where in this review, this advantage cannot be totally realized in practical spacecraft applications due to external effects. A state-of-the-art fluxgate magnetometer will exhibit zero level drift of $<0.2$ nT/yr and $<0.5$ nT over the temperature range of $-55\,°C < T < 75\,°C$. The noise performance of fluxgates is strongly affected by mechanical and thermal stresses, which vary over time and with exposure to extreme environments. These are usually at their maximum during instrument development and testing and it is common for noise performance to improve over time after the launch, particularly if exposure to the environment is constant or limited. The Voyager mission magnetometers improved their noise performance from 0.005 nT rms immediately after the launch in 1977 to 0.001 nT rms (0–1 Hz bandwidth) during the Jupiter fly-by 2 years later.

The traditional fluxgate magnetometer design shown in Fig. 3 has also evolved to include "short-circuited" fluxgates,[95,96] "digital" fluxgates,[97–99] fast Fourier transform (FFT)-based fluxgates,[97] "current output" fluxgates,[100] and many others. The basic principles remain the same, with the differences being mostly in how the error signal is processed to generate the feedback field.[101] It is difficult to assess the advantages or disadvantages of each implementation given the multiplicity of requirements and constraints associated with each space mission. However, low cost, accuracy, low power consumption, small mass and volume, large dynamic range, low noise, and good zero level stability remain the premier characteristics sought in space-based magnetometers.[8,49,76,95,102]

## IV. ELECTRON REFLECTION MAGNETOMETRY

The Mars Global Surveyor and Lunar Prospector missions included magnetic field investigations capable of making *in situ* measurements with high performance fluxgate magnetometers like those described above, as well as *remote sensing* instruments capable of deriving the intensity of the magnetic field at a significant distance from the spacecraft. The latter use the technique of *electron reflectometry*, which is based on the fact that ambient electrons, like those in the solar wind and in planetary environments, can travel along magnetic field lines and be reflected when they encounter an increase in flux density associated with a source of magnetism.[26,29,32] Thus, an electron reflectometer is an instrument that measures the flux of electrons moving along the local magnetic field lines and the "pitch angle distribution" for both directions. The presence of a magnetic source in the path of the electrons will cause them to be reflected, altering the pitch angle distribution. This information can be cast in the form of a *reflection coefficient*, which is directly proportional to the intensity of the field at the point of reflection. This sensitive technique is particularly useful in the case of the Moon where no atmosphere exists to absorb the electrons and thus surface magnetic fields can be measured from an orbiting spacecraft.[26–28] In the case of Mars, the presence of an atmosphere limits the measurement altitude to the top of the atmosphere or $\sim 100$ km although the existence of strong crustal fields limits the usefulness of this technique.[32] An important advantage of electron reflection
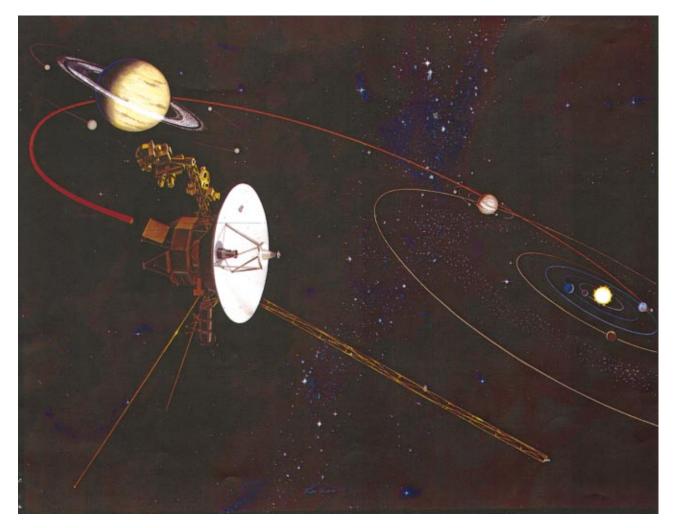
FIG. 5. (Color) Artist's illustration of the Voyager spacecraft and mission to the outer planets. The 14 m long magnetometer boom can be seen in the lower half of the picture and dominates the dimensions of the spacecraft when deployed. Four triaxial sensors are mounted on this boom, one at the tip, a second two thirds of the distance from the tip to the base, and two on the support canister.

magnetometry is the improved spatial resolution obtainable since the ''footprint'' of the electrons at the point of reflection is their Larmor radius ($<$ 2 km for lunar fields). The spatial resolution obtainable from *in situ* measurements with conventional magnetometers aboard an orbiting spacecraft is at best equivalent to the orbit altitude above the surface.

## V. ROCKETS AND SPACECRAFT AS MAGNETIC FIELD MEASUREMENT PLATFORMS

The measurement platforms for the instruments described above are spacecraft, rockets, and balloons, and they include complex systems of mechanical, electrical, and electronic components. They all have the potential of producing magnetic fields of their own and careful control techniques must be used to minimize errors introduced by these unwanted sources. Batteries, solar arrays, motors, wiring, materials, etc. must be especially designed and/or selected to minimize the generation of ''stray'' magnetic fields that will affect measurements of the ambient field. The design and implementation of a magnetically ''clean'' spacecraft that meets the stringent requirements of a high accuracy Earth-orbiting or interplanetary mission is an extremely demanding task that has tested the fiber of many seasoned project man-

agers, engineers, and scientists. Since it is practically impossible to reduce the stray spacecraft magnetic field to the smallest levels required for sensitive measurements, placement of the magnetic sensors away from the main body of the spacecraft is commonplace. This technique exploits the fact that the magnetic fields produced by finite sources decrease rapidly with distance, proportionally to $1/r^3$ as a minimum (higher order multipoles decrease even more rapidly), where $r$ is the distance to the source. The above is true when the dimensions of the source are smaller than the distance to the measurement point. Many missions use long, deployable ''booms'' or masts for this reason and they must be rigid and preserve the alignment required between the magnetic sensors and the attitude determination sensors mounted on the main spacecraft body, which imposes limits on the practical length of booms. The magnetometer boom of the twin Voyager spacecraft launched in 1977 to explore the outer planets of the solar system had a length of 14 m (42 ft) when fully deployed. An artist's illustration of the Voyager spacecraft shown in Fig. 5 gives a sense of the relative dimensions involved. For a given spacecraft design, the trade-off between boom length and level of magnetic cleanliness required in the main body and major subsystems is a major
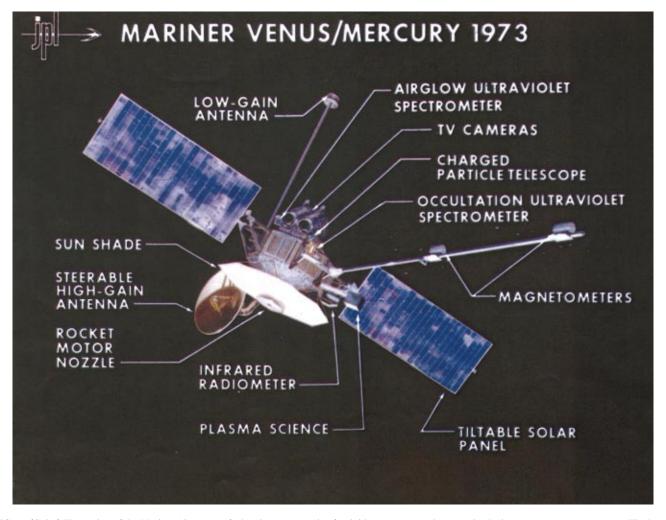
FIG. 6. (Color) Illustration of the Mariner 10 spacecraft showing an example of a rigid magnetometer boom and a dual magnetometer arrangement. The boom is 6 m long and composed of two rigid segments which deploy sequentially.

decision that must take into account many conflicting requirements, including whether the spacecraft is spin or three axis stabilized. Details on the magnetic interference control, spacecraft testing, and magnetic cleanliness programs used on early spacecraft were given in a review by Ness.[8] The early boom designs were mostly of rigid tubular type, folded against the top or side of the spacecraft in the launch configuration. To achieve longer lengths several rigid segments could be deployed sequentially, but the complexity of the mechanisms required to insure correct deployment limit the maximum number of segments to no more than three. Other boom types included "scissor" booms, helically wound booms, etc. Figure 6 shows the rigid boom used in the Mariner 10 spacecraft, while Fig. 7 illustrates the scissorstyle boom used in the MAGSAT spacecraft.

In the early 1970s a new type of truss-like, deployable boom was developed, generically called an "astromast." This very interesting structure is shown deployed in Fig. 8 and is characterized by an extremely favorable length-to-mass ratio. Three, lightweight main longerons, typically made of fiberglass, are stabilized by a series of battens and diagonal elements to form a rigid truss. In the undeployed state (Fig. 9), the longerons are coiled inside a canister mounted on the spacecraft and are prevented from deploying by a center lanyard or restraining mechanism. This lanyard is also used during deployment to control the rate at which the structure unwinds out of the canister. Booms as long as 45–50 m have been manufactured and mass-per-unit-length ratios of the order of 150 g/m are achievable. Careful control of expansion coefficients and the effect of solar illumination on the elements yield booms, which exhibit torsional and bending stability of the order of a fraction of a degree for lengths up to 10 m or more. An important consideration in computing the total mass associated with a long magnetometer boom system is the weight of the cables connecting the sensor at the tip of the boom, since the electronics are located in the main body of the spacecraft. This mass can easily exceed that of the boom itself by a significant factor. The rigidity of the sensor cables in cold temperatures and its impact on boom deployment safety margins are also critical issues, particularly in missions where successful boom deployment is a mission critical event.

The high cost of deployable booms, their potential effects on spacecraft dynamics, mission success, and magnetometer alignment, and the complexity of the associated mechanical systems limit the affordable boom length that can be realized for a given spacecraft design. The *dual magnetometer* technique was introduced in 1971 by Ness and co-
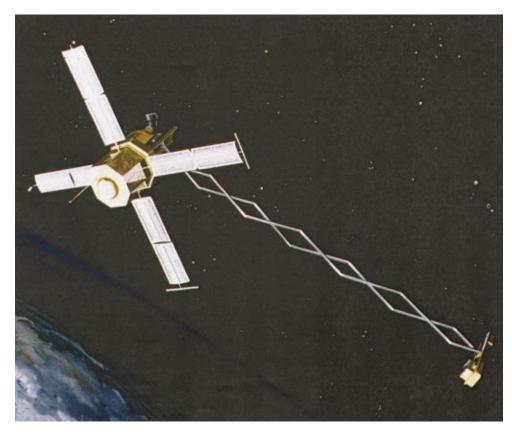
FIG. 7. (Color) MAGSAT spacecraft and its 6 m scissors boom. Optical mirrors are mounted on the magnetometer sensor platform to "transfer" its orientation to the main body of the spacecraft using infrared beams.
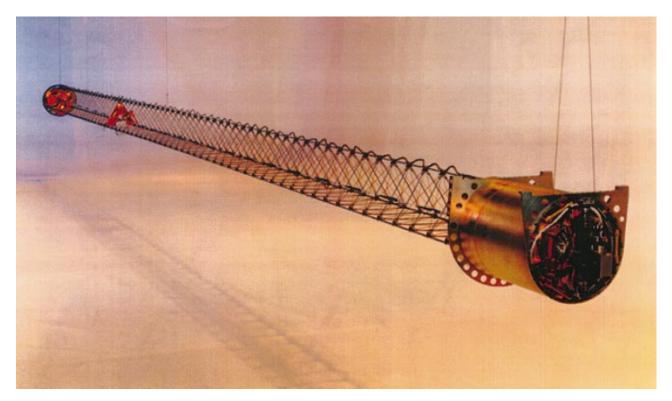


FIG. 8. (Color) Deployed astromast-style boom used in NASA's WIND and POLAR spacecraft (12 and 6 m in length, respectively) to separate the sensors from the body of the spacecraft.
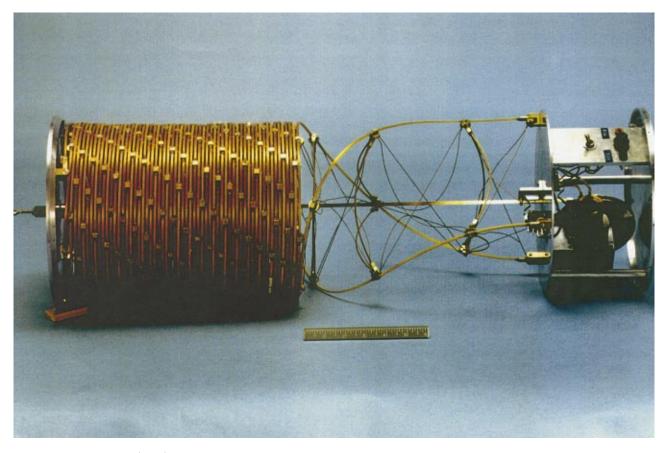
FIG. 9. (Color) Undeployed astromast-style boom showing the center lanyard and deployment mechanism.

workers to ease the problem of making sensitive magnetic field measurements in the presence of a significant spacecraft field.[103,104] This method is based on the experimental observation that beyond a certain distance most spacecraft-generated magnetic fields decrease as expected for a simple dipole source located near the center of the spacecraft ($\sim 1/r^3$). Thus it can be shown that if *two* magnetometer sensors are used, mounted along a radial boom and located at distances $r_1$ and $r_2$, respectively, it is possible to uniquely separate the spacecraft-generated magnetic field from the external field being measured. If we denote by $\mathbf{B}_1$ and $\mathbf{B}_2$ the vector fields measured at radial locations 1 and 2 with $r_2 > r_1$, the ambient field and the spacecraft field at location $r_1$ are given by

$$\mathbf{B}_{\mathrm{amb}} = (\mathbf{B}_2 - \alpha \mathbf{B}_1)/(1-\alpha), \tag{7}$$

$$\mathbf{B}_{\mathrm{s/c1}} = (\mathbf{B}_1 - \mathbf{B}_2)/(1-\alpha), \tag{8}$$

where

$$\mathbf{B}_1 = \mathbf{B}_{\mathrm{amb}} + \mathbf{B}_{\mathrm{s/c1}}, \tag{9}$$

$$\mathbf{B}_2 = \mathbf{B}_{\mathrm{amb}} + \mathbf{B}_{\mathrm{s/c2}}, \tag{10}$$

$$\mathbf{B}_{\mathrm{s/c2}} = \alpha \mathbf{B}_{\mathrm{s/c1}}, \tag{11}$$

$$\alpha = (r_1/r_2)^3. \tag{12}$$

Note that Eqs. (11) and (12) assume that the spacecraft field can be represented accurately by that due to a dipole quasicentered on the main body.

The dual magnetometer method is illustrated schematically in Fig. 10. The spacecraft-generated magnetic field decreases with distance due to the finite size of the sources, which are assumed located at the center of the spacecraft, and leads to the existence of a spatial gradient between the two magnetometer sensors. The ambient field being measured is identical at both sensors because its spatial gradient is insignificant over the dimensions of the spacecraft and boom. Thus, each sensor measures a different mixture of spacecraft and ambient field. For the special case of a *dipolar* spacecraft field, the fields due to the spacecraft at the two sensor locations are related by a simple proportionality constant. Thus, the ambient and spacecraft field can be separated
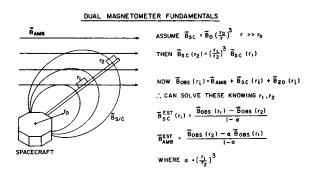


FIG. 10. Illustration of the dual magnetometer technique and associated formulas. The spacecraft-generated magnetic field ($\mathbf{B}_{\mathrm{s/c}}$) is assumed to be dipolar and centered at the body of the spacecraft while the external field ($\mathbf{B}_{\mathrm{amb}}$) is gradient-free over the separation of the sensors. $\mathbf{B}_{\mathrm{obs}}$ is the field measured which includes a constant offset $\mathbf{B}_{z0}$.

analytically as shown above. An immediate benefit of the dual magnetometer technique is that shorter booms can be used to achieve a level of accuracy equivalent to that afforded by a much longer boom. The small increase in mass represented by the second magnetometer is more than offset by the reduction in boom length and associated cabling. It is customary to see this arrangement in spacecraft used for outer solar system exploration missions where the spacecraft-generated magnetic field at the sensors may be many times larger than the weak ambient field. A particular advantage of the dual magnetometer method is that it allows unambiguous real time identification and monitoring of the *time variation* of the spacecraft-generated field. In a single magnetometer system a change in the field measured can be attributed to either a change in the spacecraft-generated field, or a change in the ambient field which leads to a unresolvable ambiguity in interpretation. Last and most important, the use of two sensors provides full measurement redundancy, which has proven essential for success in missions of long duration such as those to the outer planets.[83]

Some miniature magnetometers used for attitude determination and control integrate the fluxgate sensors and electronics into a single package. This approach is adequate if accuracy of the order of 10%–20% is acceptable, such as in momentum wheel desaturation applications. However, the proximity of the sensor to the electronics introduces additional biases and hysteresis effects and limits the environment to which the package can be exposed. Fluxgate sensors, by themselves, are capable of withstanding penetrating radiation doses of tens of megarads and temperature extremes of $-100$ to $+200\,°C$ without major difficulty, a fact that is not true for the signal processing electronics. Thus, integrated sensor-electronics instruments must be mounted within the main body of the spacecraft where temperature extremes are within operational limits but unfortunately the close proximity to many sources of stray magnetic fields, substantially limits their accuracy.

The complexity and cost of the early spacecraft magnetic control programs were truly staggering by today's standards. Special nonmagnetic materials were selected for custom-built passive and active electronic components and very often were incompatible with reliability considerations. Every spacecraft component was magnetically characterized in detail at magnetic test facilities and either *compensated for* or its design modified to use nonmagnetic parts. The Pioneer 10 and 11 spacecraft launched in 1973 to explore Jupiter and Saturn[105] were able to achieve a residual static field of less than 0.01 nT (basically, the limit in practical measurement capability at magnetic test facilities) at the end of a 3 m boom where the principal magnetometer sensor was located. Similar results were obtained for the Interplanetary Monitoring Platforms (IMP) launched to explore the Earth's magnetosphere and the interplanetary medium in the late 1960–1970s.[8]

The evolution of technology markets and spacecraft cost reduction efforts has made it impossible to implement the kind of magnetic control programs described above in contemporary space missions. Most efforts are directed towards the goal of minimizing or compensating, within available time and resources, the magnetic fields associated with existing or heritage components and systems. Current philosophy concentrates on first minimizing *time-variable* spacecraft fields associated with soft magnetic materials and circulating currents in power systems, loads, motors, actuators, solar arrays, etc. since these give rise to unknown and variable errors which are difficult to measure and remove from the data. Truly *static* fields associated with hard magnetic materials can be measured prelaunch and subtracted from the measurements assuming that they are time and temperature stable. The techniques used for static and dynamic field compensation and minimization include permanent magnets, single point grounding systems for power distribution, twisted pair wiring for all significant loads, and the use of *dummy* current loops to create equal but opposite signatures from circulating currents. Advanced computer controlled laboratory magnetometers that use synchronous sampling techniques to reject magnetic signatures at 50/60 Hz and higher power line harmonics have been developed to carry out sensitive measurements ($\sim<0.2$ nT sensitivity) in the Earth's field and in the normal environment of laboratory and spacecraft development and integration facilities. These instruments have largely eliminated the high cost and logistic complexities associated with time-consuming measurements at specialized distant magnetic test facilities. They typically incorporate real time visualization of the magnetic field data being measured, and have literally transformed spacecraft magnetic control techniques by eliminating the "black magic" aspects of the field and significantly reducing costs and complexity. It is important to emphasize that the usefulness of these measurements made in the presence of the Earth's field is limited to those applications where *induction* effects are small. When large structures made of high permeability materials, particularly those having a large length-to-diameter ratio (e.g., magnetic torquers), are present, induction effects will dominate, thereby introducing great difficulties in interpretation of the data.

Another important magnetic control tool has been added by today's widespread availability of mathematical modeling software in personal computers, which has allowed rapid numerical and/or analytical computation of the magnetic fields generated by permeable structures and different circulating current geometries. These are particularly useful in the case of solar arrays where many linear current segments and current sheets are involved and a minimal magnetic signature due to the variable circulating currents is desired. In some cases, like in the Mars Global Surveyor mission, the large size of the solar arrays ($\sim15$ m$^2$) made it possible to use them as booms to place the magnetometer sensors some 5 m from the main body of the spacecraft, at the outer edge of each panel, obviating the need for a classical deployable boom (see Fig. 11). However, that approach required that the current paths in the array and solar cells be modeled, calculated, and manufactured (to precision of 1.5 mm) to cancel out the magnetic field at each sensor location. The final contamination level achieved in Mars' orbit for the solar array contribution was $\sim0.25$ nT. This impressive performance was unfortunately compromised by the presence of large arrays of uncompensated magnets in the traveling-wave-tube
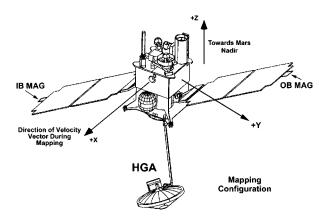
FIG. 11. Mars Global Surveyor spacecraft, solar panels, locations of magnetometer sensors (OB and IB), and high gain antenna which includes the traveling-wave-tube amplifiers and their magnet assemblies.

amplifiers (TWTAs), which were mounted on the back side of the articulated high gain antenna (HGA) (see Fig. 11), thus creating a source of time varying fields as the spacecraft orbited Mars. The magnitude of the error signal created by the TWTA magnets is illustrated in Fig. 12 where data acquired when the solar panels were being articulated is shown for each of the triaxial magnetometer sensors mounted at the edge of the solar panels ($Bx$, $By$, and $Bz$). Under ideal conditions no variations in any of the components should have been observed as a function of panel position and angle. However, the presence of the TWTA tube magnets leads to the time varying signals shown in Fig. 12, and a measurement error as large as ~9 nT, almost three times the average value of the interplanetary magnetic field of Mars. These data were acquired during special maneuvers and solar array motion designed to estimate parameters for analytical models of the spacecraft-generated field to be subtracted from the raw data.

From the foregoing, it is clear why, in a cost and schedule constrained environment, many space mission managers prefer spacecraft *without* sensitive magnetometers! Experimental success depends critically on outstanding systems engineering, close collaboration among experimental scientists, and spacecraft designers, and real management leadership.

## VI. ANALOG SIGNAL AND ONBOARD DATA PROCESSING FOR SPACE MAGNETOMETERS

The study of the frequency spectrum of dynamic perturbations of the ambient magnetic field is a powerful tool that is used to identify the type and characteristics of waves and other time variable phenomena detected by spacecraft magnetometers. Although most of the applications and research activities are concentrated in the 0 to ~10 Hz frequency range, higher frequency and time resolution data are extremely useful for identifying interaction boundaries, plasma waves, magnetohydrodynamic shocks, and other fast phenomena that take place in planetary magnetospheres and in the solar wind. Telemetry and power resources, particularly those on spacecraft traveling to the outer reaches of the solar system, are extremely limited and some form of onboard data processing is required to reduce the rate of the data transmitted to Earth. The power spectrum of naturally occur-
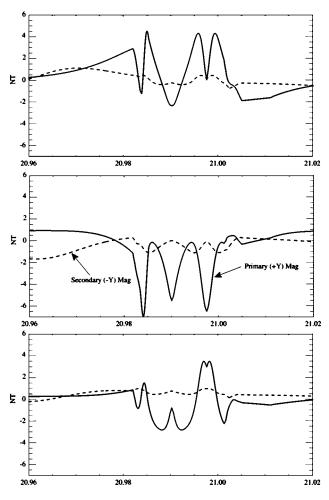


FIG. 12. Mars Global Surveyor spacecraft-generated magnetic fields introduced by the magnet assemblies in the TWTAs. Articulation of the solar panels and antenna introduces time variable signals in an otherwise relatively constant background. The primary and secondary definitions apply to the OB and IB sensors, respectively, shown in Fig. 11. The $X,Y,Z$ coordinates refer to the spacecraft's principal axes.

ring magnetic fluctuations falls off with increasing frequency roughly as ($1/f^n$) with $n$ varying approximately between 1.5 and 3 depending on the phenomena being observed. The processing and digitization of the magnetometer analog output signals for eventual transmission to Earth must therefore take into account these spectral characteristics and the desired time resolution. Analog-to-digital (A/D) conversion resolutions of 12 to >16 bits are commonly used to recover as much of the spectrum as possible without having to resort to prewhitening filters or similar spectrum-shaping techniques which increase power consumption. The availability of low power, very-high-resolution A/D converters, such as those using sigma–delta techniques, has allowed the simplification of earlier instrument designs that resorted to complex step-biasing techniques to achieve higher resolution than that obtainable with 8–12 bit A/D converters.[8,32,45,46,79,90,106]

To prevent aliasing errors the magnetometer output must be sampled at least twice as fast as the highest frequency of interest (the Nyquist rate), a fact that coupled to the high digital resolution required results in the generation of voluminous amounts of raw digital data onboard. These data cannot be transmitted directly to Earth because of telemetry and communication system limitations and intelligent data pro-

cessing techniques and algorithms are used to implement data compression and extraction of information from the on-board raw data. Many forms of data compression, both loss-less and lossy, have been used to increase the information content per magnetometer bit transmitted to the ground. Averaging and/or data differencing between adjacent samples with periodic baseline recovery is the least complex method and is easily implemented with simple logic algorithms. For a typical magnetic field power spectrum it achieves compression factors in the range of 2–5 without major penalties or storage requirements and hence it is often used in data rate limited missions where accurate inversion of the compressed signal with minimal spectral distortion is an important objective. At the other extreme, complex adaptive lossless algorithms exist which can achieve compression factors in the range of 10–100 but require significant onboard storage and processing capabilities and extremely careful time synchronization management. It is important to emphasize that the greater the compression efficiency (or entropy per bit) the greater the sensitivity of the system to bit errors introduced by communication channel performance which may or may not be correctable. Where significant light-trip times are involved, retransmission of data packets (as in ground data networks) is not an option since space magnetometers generally require the acquisition of continuous data streams without significant gaps and fixed data rate allocations are commonplace. Typical effective data rates for spacecraft magnetic field experiments may range from a few bits per second to 2 kbits/s or more while for rockets and balloons rates of up to several tens of kbits/s are common for direct links.

Onboard spectrum analyzers based on FFT algorithms have been used in advanced magnetic field experiments like the one developed for the WIND and ACE spacecraft.[45,46] The availability, starting in the early 1980s, of high reliability, low power digital signal processor chips and radiation hardened memories made possible the efficient implementation of FFT engines to process high sample rate magnetometer data on board spacecraft. Since the magnetometer data consist of three simultaneous time series that correspond to the three orthogonal components of the field, each one must be stored and processed independently. Phase information is important, hence both real and imaginary components of the power spectral matrix are preserved to compute auto- and cross-spectral power densities as a function of frequency. In general, logarithmic frequency scales are desired and these must be synthesized from the resulting linear FFT transformation. A number of real time and/or frequency domain data weighting windows are also implemented to attenuate the spectral contamination effects of discrete length data sets.

Spinning spacecraft are usually preferred for simple attitude stabilization and studies of the plasma and charged particle space environment if full solid angle coverage by the instruments is desired. The spinning motion of the spacecraft sweeps the limited field of view of particle instruments through solid angle space to achieve a much larger spatial sampling of the charged particle population (the distribution function). Since the magnetometer is fixed to the body of the spacecraft or to the boom and one of its sensing axes is usually aligned with the spin axis, the magnetic field components in the spin plane will exhibit large amplitude modulation at the spin frequency. This requires that additional bandwidth be provided to the magnetometer to resolve the spin frequency accurately and avoid aliasing, or that spin modulation be removed on board prior to data compression and transmission to the ground. The same applies if onboard FFT-based spectral analysis is used: the large amplitude spin induced signals must be removed from the data prior to FFT processing to avoid spectral leakage and dynamic range problems in digital signal processor (DSP) algorithms. Modern space-based magnetometers like those on the WIND and ACE spacecraft incorporate data de-spinning capabilities in their digital processing units[45] as part of the onboard FFT processor. The de-spinning algorithm utilizes onboard information on the spin rate and spin phase to transform the magnetic field data to a coordinate system aligned with a reference direction, usually the Sun.

The attractive advanced onboard computational capabilities provided by today's microprocessors, DSPs, and large memories have to be traded off against the costs and complexities associated with the space environment, the availability of high reliability components, fault-tolerant software development, and testing costs. The high radiation environment associated with orbits where spacecraft spend a significant amount of time in the radiation belts or missions to Jupiter like Voyager and Galileo severely limits the types of devices that can be considered for flight instruments. Latchup and single-event upsets in memories, processors, and complex logic devices must also be considered in designing magnetic field instruments for space applications. The radiation protection afforded by the spacecraft bus, fuel tanks, and subsystems can be substantial and is usually taken into account in trade-off studies. Magnetometers with separate sensors and electronics can take full advantage of this protection since the sensors are typically much more radiation tolerant than the electronics and are placed on booms far from the main body of the spacecraft for magnetic contamination reasons.

## VII. PRE-LAUNCH AND IN-FLIGHT CALIBRATION AND ALIGNMENT TECHNIQUES

Accurate calibration of space-based magnetometers with a dynamic range of a few nanoteslas to hundreds of thousands of nanoteslas full scale presents unique problems which require special techniques and facilities. Among the many issues involved, the following are typical.

(1) Shielding or cancellation of the Earth's magnetic field and the generation of accurately known magnetic fields (magnitude and direction) including very weak fields, "true zero field," and the minimization of thermoelectrically induced magnetic fields caused by temperature gradients. The typical frequency range considered is 0 to 25–50 Hz.

(2) The extreme environmental range over which the magnetic field sensors and their electronics must operate and be characterized (temperature, pressure, radiation, vibration, shock). The parameters of interest are, at a mini-
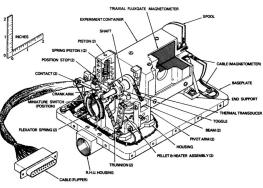
FIG. 13. (Color) Voyager magnetometer boom, supports, and magnetic shields during spacecraft integration and tests. The shields are required to attenuate the Earth's field (~31 000 nT) so test measurements in the most sensitive range (±8 nT) can be made.

mum, noise, zero level, scale factor, and dynamic response for each magnetometer dynamic range. Depending on the complexity of the associated onboard analog and digital processing units, many additional functions and parameters are typically monitored and characterized.

(3) Determination of the angular alignment of the sensors with respect to an external reference coordinate system over the environment defined in (2) and in controlled magnetic fields defined at the beginning of Sec. II.

(4) Determination, calibration or elimination of induced magnetization effects caused by the presence of components with ferromagnetic materials of high relative permeability (e.g., electromagnet cores). Although the material may not contribute significantly to the stray field its permeability distorts the geometry of the ambient field sensed by the magnetometer.

The cost and complexity of the calibration and spaceflight qualification activities for space magnetometers can match and exceed those of their development and manufacturing phase. For this reason "heritage" instruments that have already demonstrated their capabilities and limitations over many space missions are usually preferred since many of these tests can be simplified or eliminated. The most demanding calibration programs are those associated with ultrahigh accuracy instruments designed to map the Earth's magnetic field[77,79,81] where the absolute magnitude and angular accuracy required are of the order of 1–2 parts in

100 000 and a few arcsec, respectively. Figure 13 illustrates some of the complexities associated with integration activities that involve long magnetometer booms, in this case that of the Voyager spacecraft. The large structures are not designed to be self-supporting in the Earth's gravitational field and relatively complex mechanical support equipment must be used to deploy them.

It is a well-known fact that the launch environment and the transition to the mission phase environment always result in minor shifts in magnetometer calibration and performance parameters except where absolute instruments are involved. It therefore becomes necessary to apply in-flight calibration techniques that have been developed to recover accurate estimates of the true performance parameters for a given space-based instrument. To this end, spacecraft attitude maneuvers constitute a powerful calibration and verification tool. They can be used effectively to establish effective zero levels and sensor alignment with respect to the reference axes.[43,107] Spinning spacecraft are particularly good for the estimation of zero levels for the two magnetic field components in the spin plane and the angular alignment of the component parallel to the spin axis. In many three-axis-stabilized spinning spacecraft, mechanical sensor "flippers" are used to rotate the fluxgate sensors through 90° or 180° and thus establish the effective zero level of the sensors (see Fig. 14). This mechanical rotation is equivalent to inverting the leads in a bipolar voltmeter to determine its zero offset. Typical devices used to develop the mechanical force needed to rotate the

FIG. 14. Mariner Jupiter–Saturn 77 (Voyager) sensor mechanical flipper assembly used initially to establish zero offsets. Heated wax pellet actuators, similar to automobile radiator thermostats, develop the force that causes the sensor assembly to rotate (flip) without generating a significant magnetic field. Radioisotope heater units (RHUs) are used to maintain the sensor temperature within its operating range.

assembly without generating a magnetic field include wax pellets or bimetal strips. For Earth-orbiting magnetometers many calibration parameters can be derived by comparing the actual measurements to available models of the geomagnetic field[49] and deriving least-squares fitted correction algorithms. Magnetometers on interplanetary spacecraft do not benefit from the availability of accurate models of the interplanetary magnetic field which is extremely time varying. However, many years of observation have shown that most of this variability is in the angular direction and not in the field magnitude. It is possible then to formulate a statistical least-squares estimation algorithm for magnetometer zero level errors. If we denote the true ambient magnetic field at two instants of time as $\mathbf{B}_{a1}$ and $\mathbf{B}_{a2}$ and the field measured by the magnetometer at those same times as $\mathbf{B}_{m1}$ and $\mathbf{B}_{m2}$, respectively, we can write

$$\Delta\mathbf{B} = \mathbf{B}_{m2} - \mathbf{B}_{m1}, \tag{13}$$

and, because of the assumptions discussed above,

$$0.5(\mathbf{B}_{a1} + \mathbf{B}_{a2}) \cdot \Delta\mathbf{B} = 0. \tag{14}$$

The fields measured are given by

$$\mathbf{B}_{m1} = \mathbf{B}_{a1} + \mathbf{Z} \quad \text{and} \quad \mathbf{B}_{m2} = \mathbf{B}_{m2} + \mathbf{Z}, \tag{15}$$

where $\mathbf{Z}$ denotes the "offset" vector due to bias in the magnetometer electronics and stray fields generated by the spacecraft. We call this the "effective zero" of the magnetometer. We can estimate the value of $\mathbf{Z}$ in a least-squares sense from a series of vector measurements ($i = 1,2,3,....,n$) where the ambient magnetic field has primarily changed direction and perhaps magnitude "adiabatically" as follows:

$$0.5(\mathbf{B}_{mi} + \mathbf{B}_{m(i+1)}) \cdot \Delta\mathbf{B}_i = \mathbf{Z} \cdot \Delta\mathbf{B}_i, \tag{16}$$

$$\mathbf{Z} = [0.5(\mathbf{B}_{mi} + \mathbf{B}_{m(i+1)})\Delta\mathbf{B}_i][\Delta\mathbf{B}_i]^{-1}, \quad i = 1,2,3,...,n, \tag{17}$$

where the matrices shown have been computed from the time series of data. A minimum of three data points is needed to estimate $\mathbf{Z}$ in two dimensions, such as the offsets in the spin plane for a spinning spacecraft, while four or more measure-ments are needed for the three-dimensional case. The nonsquare inverse matrix $[\Delta\mathbf{B}_i]^{-1}$ is usually computed by pseudoinverse techniques.

The least-squares estimation problem described above is representative of a whole family of similar techniques that have been developed to estimate parameters associated with magnetic field measurements "in flight." If highly accurate models of the ambient field are available, as in the case of the Earth, effective scale factors, angular alignment, and zero biases are estimated routinely for many space missions. Where interplanetary and magnetospheric missions are concerned the estimation of effective zero levels usually constitutes a major continuing calibration effort due to spacecraft effects and their variability. Scale factors are monitored through built-in instrument calibration capabilities using step functions from precision current sources and absolute accuracy better than 0.1%–0.25% is seldom required. In some instances, it is difficult to simulate zero-$G$ conditions during testing on the ground and boom alignment angles are not known to the desired accuracy (Fig. 12). Lightweight, large diameter coils, usually wound around a parabolic antenna structure, have been used[83] to generate calibration magnetic fields whose direction is known precisely and allow the determination of in-orbit alignment angles. A single coil allows the estimation of only two orientation angles and two coils mounted orthogonal to each other are required for estimation of the full set of alignment angles. However most long booms exhibit preferential distortion about a single axis (torsion or bending) and a single coil is usually satisfactory.

## VIII. COORDINATE SYSTEMS

Generally, to carry out the research intended the measurements must be expressed in a physical coordinate system, which is different from that of magnetic field sensors.[52,108] Therefore, coordinate transformations are required which must take into account not only the orientation of the spacecraft in inertial space, but also the internal rotations associated with booms and other instruments and sensors aboard. A simplified general expression for the desired magnetic field quantities described in a reference coordinate system and starting with the magnetometer output voltages in three channels [$\mathbf{V}$] can be given as

$$\mathbf{B} = [\mathbf{k}][\mathbf{V} - \mathbf{Z}][\mathbf{M}_{\text{sensor}}][\mathbf{M}_{\text{boom}}][\mathbf{M}_{\text{s/c inert}}], \tag{18}$$

where $\mathbf{B}$ is the measured magnetic field expressed in the coordinate system desired, $\mathbf{Z}$ is the effective zero level of the magnetometer including the A/D converter and spacecraft contributions, $\mathbf{k}$ is a vector whose components are the magnetometer scale factors and A/D converter factors for each axis, $\mathbf{M}_{\text{sensor}}$ is a nonorthogonal matrix that transforms the measurements obtained in the physical sensor system to an orthogonal system defined in the sensor frame, $\mathbf{M}_{\text{boom}}$ is an orthogonal matrix that transforms the measurements from the sensor frame to the frame of the body of the spacecraft where inertial references are located, and $\mathbf{M}_{\text{s/c inert}}$ is an orthogonal matrix that relates the spacecraft inertial reference frame to the reference frame desired. It is clear that the ultimate accuracy achievable in magnetic field measurements depends

strongly on precise knowledge of these parameters, many of which are closely related to system level performance characteristics. Scalar measurements are obviously insensitive to coordinate transformation issues and are concerned only with spacecraft magnetic contamination levels.

## IX. THE FUTURE

The preceding discussion has illustrated the significance of space-based magnetic field measurements and their relevance, not only for space physics research and planetary exploration, but also for the emerging field of space weather prediction and quantitative assessment of the geoeffectiveness of solar-terrestrial events.[53] Engineering applications in low and geostationary orbit will continue to take advantage of the reliability, simplicity, and low cost of magnetometers as attitude sensors and a control element for magnetic torquing systems. Fluxgate magnetometers are expected to continue to dominate the field although recent improvements in magnetoresistance technology will certainly have an impact on high volume applications such as spacecraft constellations used for communications from Earth's orbit where absolute accuracy may not be a primary requirement. In the area of space research applications, a significant shortage of low noise, high permeability materials, such as those in the Permalloy family, is a source of concern. The widespread use of ferrites as magnetic core materials in industrial and commercial applications, with their significant cost and performance advantages, has caused the almost total disappearance of U.S. manufacturers of tape-wound cores and specialty nickel–iron–molybdenum alloys used in high performance fluxgate sensors. The increasing use of amorphous metallic glasses to replace Permalloys[49,109,110] is a compromise since their lower Curie temperature ($<300$ vs $>600\,°C$) implies poorer temperature stability. Specialized temperature annealing of these alloys to improve noise performance does not always result in better temperature stability. The market for research grade instruments is extremely limited and it is not expected that recovery of the high-grade Permalloy production capabilities of the 1970s will take place any time soon. Limited high-grade Permalloy production capabilities exist in Europe and Japan but their future is probably just as uncertain as it is in the US.

The current trend of spacecraft miniaturization constitutes another significant problem for sensitive, research-grade, magnetic field measurements. In addition to the significant decrease in signal-to-noise-ratio resulting from reduced sensor dimensions, as the spacecraft size is reduced the distance from the sensor to the sources of unwanted fields is also reduced, and their effect amplified as $\sim(r_0/r)^3$ where $r_0$ denotes the reference distance and $r$ the reduced distance to the source. The overall reduction in spacecraft power consumption with miniaturization is not sufficient at present to compensate for the deleterious effects of the proximity of the sources. In principle, custom spacecraft and subsystem designs that take into account magnetic field measurement objectives could result in acceptable performance but are ruled out by cost considerations. Low cost, commercial-off-the-shelf (COTS) subsystems are not neces-

sarily designed with sensitive magnetics performance requirements in mind. The current stock of high performance grade, fluxgate sensor materials will be exhausted in the near future, just when spacecraft constellation programs involving perhaps hundreds of spacecraft (Magnetospheric Multi-Scale, SWARM, ANTS, etc.) are supposed to be coming on line. Unless a significant investment is made to recover production capabilities for high-grade Permalloys, the performance of magnetometers aboard these missions will fall far short of the requirements for ''world-class'' science and engineering.

## NOMENCLATURE

The following are space mission acronyms used in the text.

ACE—Advanced Composition Explorer, NASA Explorer mission launched in August of 1997 to measure and compare the elemental and isotopic composition of the solar corona and to monitor the interplanetary medium.

ANTS—Autonomous Nano-Technology Swarm, a fleet of miniature spacecraft that would cruise independently to the Asteroid Belt. Each probe would hoist its own solar sail to capture the minute pressure of the Sun's rays.

BEPPI COLOMBO—A joint mission by the European Space Agency (ESA) and Japan's Institute for Space and Astronautical Science (ISAS) to explore the planet Mercury. It will be launched in the near future.

CASSINI mission—This spacecraft was launched by NASA in 1997 to explore the Saturn system beginning in 2004.

CLUSTER II—An ESA mission consisting of four identical spacecraft launched in the summer of 2000 to explore near-Earth space.

DEEP SPACE 1—A NASA New Millenium Mission launched in October 1998 to demonstrate new space technologies in propulsion and guidance.

GALILEO—The GALILEO spacecraft was launched by NASA in October of 1989 to carry out a 2 year detailed exploration of Jupiter, its moons, and environment.

GEOTAIL—The GEOTAIL mission is a collaborative project by Japan's ISAS and the National Aeronautics and Space Administration (NASA). Its primary objective is to study the dynamics of the Earth's magnetotail over a wide range of distances. It is also part of the International Solar Terrestrial Physics Program.

GIOTTO—An ESA mission named after the Italian artist Giotto and launched in July of 1985 to encounter the comet Halley.

HELIOS—A joint NASA–Federal Republic of Germany project consisting of two spacecraft (Helios 1 and Helios 2) launched in 1974 and 1976 to explore interplanetary space close to the Sun ($\sim$0.4 AU).

INTERPLANETARY MONITORING PLATFORM (IMP)—IMP-8 was launched by NASA on October 26, 1973 to measure the magnetic fields, plasmas, and energetic charged particles of the Earth's magnetotail and magnetosheath and of the near-Earth solar wind. IMP-8 was the last of 10 IMP spacecraft launched over 10 years.

LIVING WITH A STAR (LWS)—This is a space-weather

focused, applications-driven NASA research program. Its goal is to develop scientific understanding of those aspects connected with the Sun–Earth system that directly affect life and society.

LUNAR PROSPECTOR—A NASA Discovery mission launched in January of 1998 to orbit the Moon and map its surface composition and polar ice deposits, and measure magnetic and gravity fields.

MAGNETOSPHERIC MULTI-SCALE (MMS)—A fleet of four spacecraft similar to CLUSTER designed to study the Earth's magnetosphere. This mission is part of the NASA Solar Terrestrial Probes program.

MAGSAT—The Magsat project was a joint NASA/U.S. Geological Survey (USGS) effort to map near-Earth magnetic fields on a global basis. The spacecraft was launched in October 1979 and re-entered the Earth's atmosphere six months later.

MARINER missions—A series of NASA missions launched since the early 1960s designed to explore the interplanetary medium and the terrestrial planets. The last spacecraft in the series were the twin Mariner Jupiter–Saturn probes launched in 1977 later renamed Voyagers 1 and 2 (see below).

MARS GLOBAL SURVEYOR—A NASA Mars exploration mission launched in 1996 to map the red planet and study is topography, magnetic field, and gravity.

MESSENGER—A NASA Discovery mission to explore the planet Mercury to be launched in 2003.

NEAR-SHOEMAKER Mission—The Near-Earth Asteroid Rendezvous Mission (NEAR) was launched by NASA in February of 1996 to rendezvous with the Asteroid Eros 433 and orbit this object for 1 year to conduct imaging, gravity, and magnetic field studies.

ØERSTED—The main purpose of the ØRSTED satellite is to provide precise global mapping of the Earth's magnetic field. This small spacecraft was built by Denmark and launched as a secondary payload in January 1999 aboard a U.S. rocket.

PIONEER missions—A series of NASA low cost missions designed to explore the interplanetary medium, our Sun's environment, and the planets Jupiter, Saturn (Pioneers 10 and 11), and Venus (Pioneer Venus). The last Pioneer mission (13) was launched in 1978.

SOLAR TERRESTRIAL PROBES—A six mission NASA program to study the Earth's magnetosphere, the atmosphere/ionosphere system, the Sun, and the interplanetary medium.

SWARM—SWARM will be placed into orbit around asteroid Ceres. From this vantage point, its instrumentation will be able to study the asteroid at close range. Its primary mission will be to observe Ceres and transmit its observations back to Earth.

ULYSSES—A joint NASA–ESA mission named after the Greek hero to chart the unexplored regions above and below the Sun and the ecliptic plane. It was launched in October of 1990 from the Space Shuttle.

VOYAGER (Voyagers 1 and 2)—The twin Voyager spacecraft were launched by NASA in 1977 (as Mariner Jupiter–Saturn probes) to explore the planets Jupiter and Saturn. The mission was later expanded to encompass the exploration of all the outer planets with the exception of Pluto.

WIND and POLAR Missions—The WIND and POLAR spacecraft are part of the ISTP to study Solar-Terrestrial Physics. They were launched in 1994 and 1996, respectively.

[1] Sh. Sh. Dolginov and N. V. Pushkov, Dokl. Akad. Nauk USSR **129**, 77 (1959).
[2] Sh. Sh. Dolginov, L. N. Zhuzgov, and N. V. Pushkov, Artificial Earth Satellites **2**, 63 (1959).
[3] Sh. Sh. Dolginov, L. N. Zhuzgov, and V. A. Selyutin, Iskusstvennyye Sputniki Zemli **4**, 135 (1960).
[4] C. P. Sonnet, J. Geophys. Res. **68**, 1229 (1963).
[5] J. P. Heppner et al., Space Res. **1**, 982 (1960).
[6] L. J. Cahill, *Space Physics* (1964), pp. 301–349.
[7] N. F. Ness, J. Geophys. Res. **70**, 2989 (1965).
[8] N. F. Ness, Space Sci. Rev. **11**, 459 (1970).
[9] N. F. Ness et al., Science **233**, 85 (1986).
[10] N. F. Ness et al., Science **246**, 1473 (1989).
[11] J. E. P. Connerney, M. H. Acuña, and N. F. Ness, J. Geophys. Res., [Solid Earth Planets] **92**, 15234 (1987).
[12] J. E. P. Connerney, M. H. Acuña, and N. F. Ness, J. Geophys. Res., [Solid Earth Planets] **96**, 19023 (1991).
[13] C. T. Russell, R. C. Elphic, and J. A. Slavin, J. Geophys. Res. **85**, 8319 (1980).
[14] N. F. Ness, Annu. Rev. Earth Planet Sci. **7**, 249 (1979).
[15] S. C. Solomon, New Sci. **165**, 2223 (2000).
[16] D. MacKenzie, New Sci. **168**, 2261 (2000).
[17] Sh. Sh. Dolginov, L. N. Zhuzgov, and S. I. Shkolnikova, Kosm. Issled. **22**, 792 (1984).
[18] J. G. Luhmann, Rev. Geophys. **29**, 965 (1991).
[19] W. Riedler et al., Nature (London) **341**, 604 (1989).
[20] M. H. Acuña et al., Science **279**, 1676 (1998).
[21] M. H. Acuña et al., Science **284**, 790 (1999).
[22] J. E. P. Connerney et al., Science **284**, 794 (1999).
[23] A. B. Binder, Science **281**, 1475 (1998).
[24] G. S. Hubbard et al., Acta Astronaut. **41**, 585 (1997).
[25] G. S. Hubbard, A. B. Binder, and W. Feldman, IEEE Trans. Nucl. Sci. **45**, 880 (1998).
[26] R. P. Lin et al., EOS Trans. Am. Geophys. Union **55**, 1181 (1974).
[27] R. P. Lin et al., Science **281**, 1480 (1998).
[28] J. E. McCoy et al., EOS Trans. Am. Geophys. Union **56**, 1012 (1975).
[29] K. A. Anderson et al., EOS Trans. Am. Geophys. Union **56**, 1012 (1975).
[30] L. L. Hood et al., Phys. Earth Planet. Inter. **20**, 291 (1979).
[31] L. L. Hood et al., Geophys. Res. Lett. **26**, 2327 (1999).
[32] M. H. Acuña et al., J. Geophys. Res., [Planets] **97**, 7799 (1992).
[33] M. H. Acuña et al., J. Geophys. Res., [Planets] **102**, 23751 (1997).
[34] A. Balogh et al., Astron. Astrophys., Suppl. Ser. **92**, 221 (1992).
[35] M. G. Kivelson et al., Space Sci. Rev. **60**, 357 (1992).
[36] M. G. Kivelson et al., Science **261**, 331 (1993).
[37] F. M. Neubauer et al., J. Phys. E **20**, 714 (1987).
[38] I. Richter et al., Geophys. Res. Lett. **28**, 1913 (2001).
[39] C. T. Russell et al., IEEE Trans. Geosci. Remote Sens. **18**, 32 (1980).
[40] E. J. Smith, Adv. Space Res. **13**, 5 (1993).
[41] J. E. Smith and C. P. Sonnett, IEEE Trans. Geosci. Electron. **GE-14**, 154 (1976).
[42] M. H. Acuña et al., Icarus **155**, 220 (2002).
[43] B. J. Anderson et al., IEEE Trans. Geosci. Remote Sens. **39**, 907 (2001).
[44] D. A. Lohr et al., Johns Hopkins APL Tech. Dig. **19**, 136 (1998).
[45] R. P. Lepping et al., Space Sci. Rev. **71**, 207 (1995).
[46] C. W. Smith et al., Space Sci. Rev. **86**, 613 (1998).
[47] R. C. Snare, in *Measurement Techniques in Space Plasmas*, edited by R. Pfaff, Geophysical Monograph No. 103 (American Geophysical Union, 1998), pp. 101–115.
[48] J. S. Eterno, in *Space Mission Analysis and Design*, 3rd ed., edited by J. R. Wertz and W. L. Larson (Kluwer Academic–Microcosm Press, 1999).
[49] P. Ripka, *Magnetic Sensors and Magnetometers* (Artech House, Dedham, MA, 2001).
[50] M. Shuster, in *Fundamentals of Space Systems*, edited by V. L. Pisacane and R. Moore (Oxford University Press, Oxford, 1994).
[51] M. H. Acuña et al., Space Sci. Rev. **71**, 5 (1995).
[52] W. H. Mish et al., Space Sci. Rev. **71**, 815 (1995).
[53] D. N. Baker, Solar-Terrestrial Relations: Predicting The Effects On The Near-Earth Environment **22**, 7 (1998).
[54] N. C. Maynard, Rev. Geophys. **33**, 547 (1995).

[55] M. A. Shea and D. F. Smart, Solar-Terrestrial Relations: Predicting The Effects on The Near-Earth Environment **22**, 29 (1998).

[56] D. F. Webb, IEEE Trans. Plasma Sci. **28**, 1795 (2000).

[57] R. Pirjola *et al.*, Phys. Chem. Earth **25**, 333 (2000).

[58] D. N. Baker, IEEE Trans. Plasma Sci. **28**, 2007 (2000).

[59] D. N. Baker and J. G. Kappenman, Science **273**, 168 (1996).

[60] J. G. Kappenman and V. D. Albertson, IEEE Spectrum **27**, 27 (1990).

[61] V. D. Albertson *et al.*, IEEE Trans. Power Deliv. **8**, 1206 (1993).

[62] A. Balogh *et al.*, Space Sci. Rev. **79**, 65 (1997).

[63] S. Kokubun *et al.*, J. Geomagn. Geoelectr. **46**, 7 (1994).

[64] M. W. Dunlop *et al.*, Planet. Space Sci. **47**, 1389 (1999).

[65] D. Duret *et al.*, IEEE Trans. Magn. **31**, 3197 (1995).

[66] D. Duret *et al.*, IEEE Trans. Magn. **32**, 4935 (1996).

[67] H. Aschenbrenner and G. Goubau, Hochfreq Tech. Electroakust **47**, 178 (1936).

[68] J. Nickel, Report No. HPL-95-60, 1995.

[69] F. Primdahl, J. Phys. E **12**, 241 (1979).

[70] N. Kernevez and H. Glenat, IEEE Trans. Magn. **27**, 5402 (1991).

[71] R. E. Slocum and F. N. Reilly, IEEE Trans. Nucl. Sci. **NS-10**, 165 (1963).

[72] R. E. Slocum, P. C. Cabiness, and S. L. Blevins, J. Phys. E **42**, 763 (1971).

[73] R. E. Slocum, Phys. Rev. Lett. **29**, 1642 (1972).

[74] W. H. Farthing and W. C. Folz, Rev. Sci. Instrum. **38**, 1023 (1967).

[75] A. M. A. Frandsen *et al.*, IEEE Trans. Geosci. Remote Sens. **16**, 195 (1978).

[76] M. H. Acuña, IEEE Trans. Magn. **MAG-10**, 519 (1974).

[77] M. H. Acuña *et al.*, NASA Rep. No. TM-79656, 1978.

[78] H. Luhr *et al.*, IEEE Trans. Geosci. Remote Sens. **23**, 259 (1985).

[79] O. V. Nielsen *et al.*, Meas. Sci. Technol. **6**, 1099 (1995).

[80] W. Magnes *et al.*, Meas. Sci. Technol. **9**, 1219 (1998).

[81] J. M. G. Merayo *et al.*, Meas. Sci. Technol. **11**, 120 (2000).

[82] R. L. McPherron and R. C. Snare, IEEE Trans. Geosci. Remote Sens. **16**, 134 (1978).

[83] K. W. Behannon *et al.*, Space Sci. Rev. **21**, 235 (1977).

[84] O. V. Nielsen *et al.*, Sens. Actuators A **59**, 168 (1997).

[85] F. Primdahl and P. Jensen, J. Phys. E **15**, 221 (1982).

[86] C. P. Escoubet, C. T. Russell, and R. Schmidt, Space Sci. Rev. **79** (1997).

[87] W. A. Geyger, *Non-Linear Magnetic Control Devices* (McGraw-Hill, New York, 1964).

[88] R. L. Mcpherron, P. J. Coleman, and R. C. Snare, IEEE Trans. Aerosp. Electron. Syst. **11**, 1110 (1975).

[89] T. A. Potemra, L. J. Zanetti, and M. H. Acuña, IEEE Trans. Geosci. Remote Sens. **23**, 246 (1985).

[90] C. T. Russell, IEEE Trans. Geosci. Electron. **E-16**, 239 (1978).

[91] C. T. Russell *et al.*, Space Sci. Rev. **71**, 563 (1995).

[92] R. C. Snare and J. D. Means, IEEE Trans. Magn. **13**, 1107 (1977).

[93] D. J. Southwood, W. A. C. Mierjedrzejowicz, and C. T. Russell, IEEE Trans. Geosci. Remote Sens. **23**, 301 (1985).

[94] L. Zanetti *et al.*, Space Sci. Rev. **70**, 465 (1994).

[95] F. Primdahl *et al.*, J. Phys. E **22**, 1004 (1989).

[96] F. Primdahl *et al.*, Meas. Sci. Technol. **2**, 1039 (1991).

[97] E. B. Pedersen *et al.*, Meas. Sci. Technol. **10**, N124 (1999).

[98] J. Piilhenriksen *et al.*, Meas. Sci. Technol. **7**, 897 (1996).

[99] F. Primdahl *et al.*, Meas. Sci. Technol. **5**, 359 (1994).

[100] P. Ripka and F. Primdahl, Sens. Actuators A **82**, 161 (2000).

[101] P. Ripka *et al.*, Sens. Actuators A **46**, 307 (1995).

[102] F. Primdahl and P. A. Jensen, J. Phys. E **20**, 637 (1987).

[103] N. F. Ness *et al.*, J. Geophys. Res. **76**, 3564 (1971).

[104] R. P. Lepping, K. W. Behannon, and N. F. Ness, EOS Trans. Am. Geophys. Union **55**, 410 (1974).

[105] C. F. Hall, Science **188**, 445 (1975).

[106] M. H. Acuña, Radio Electron. Eng. **52**, 431 (1982).

[107] W. M. Farrell *et al.*, IEEE Trans. Magn. **31**, 966 (1995).

[108] C. T. Russell, Cosm. Electrodyn. **2**, 184 (1971).

[109] B. B. Narod *et al.*, Can. J. Phys. **63**, 1468 (1985).

[110] B. B. Narod and J. R. Bennest, Phys. Earth Planet. Inter. **59**, 23 (1990).